

Imaging Candida Infections in the Host

Dharmika H. Navarathna, David D. Roberts, Jeeva Munasinghe,
and Martin J. Lizak

Abstract

Disseminated fungal infections caused by *Candida* species are associated with homing of the pathogen to specific organs in human and murine hosts. Kidneys are a primary target organ of *Candida albicans*, and invasion into the kidney medulla can lead to loss of renal function and death. Therefore, development of noninvasive methods to assess kidney infections could aid in the management of disseminated candidemia. We describe a magnetic resonance imaging method utilizing iron oxide-based contrast agents to noninvasively assess recruitment of phagocytes and kidney inflammation. *C. albicans* also colonizes the brain and can cause meningoencephalitis. We describe additional imaging methods to assess loss of the blood–brain barrier function that initiates brain infections.

Key words *Candida albicans*, Noninvasive imaging, Magnetic resonance imaging, Blood–brain barrier, Kidney, Brain, Phagocytes, Inflammation

1 Introduction

Several aspects of human disseminated candidiasis can be effectively modeled in mice and have contributed much to our present understanding of the pathogenesis of *Candida albicans* infections and host immune responses to infection [1]. Kidney and brain are the primary target organs of this organism during disseminated blood-borne infections. Within the kidney, massive fungal invasion and growth can occur, resulting in inflammatory reactions that lead to tissue necrosis [2]. *C. albicans* also invades the brain during acute infections and causes meningoencephalitis [3]. Fifty percent of patients with disseminated candidiasis have central nervous system (CNS) fungal invasion, which is associated with a mortality rate reaching 90 % [4, 5]. *Candida* is the second most common contaminant cause of brain abscess formation as a result of hematopoietic stem cell transplantation [6]. *C. albicans* has also been reported to cause meningoencephalitis without systemic infection in healthy individuals [7]. Brain infection results in micro-abscesses,

mostly in the junctional area between white and gray matter. The basal ganglia and other cerebral regions are frequently involved [4]. These micro-abscesses are surrounded by inflammatory cells. Therefore, monitoring inflammatory changes and breaching of the blood–brain barrier (BBB) is an important element of *C. albicans* pathogenesis studies. Breaching of the BBB and inflammatory cell infiltration due to *Candida* infections can be effectively monitored using magnetic resonance imaging (MRI) [8].

Many biologically active nuclei (e.g., ^{31}P , ^{13}C , ^{23}Na) satisfy the conditions to perform MRI and among them, protons (^1H) are the main component of biological water, and due to its higher natural abundance and MR sensitivity ^1H is the default choice for biological MRI. The MRI signal is firstly a function of the separation of the nuclear energy levels in the presence of the main magnetic field of the scanner. Secondly, the signal depends on the complex interplay of the excitation of protons using external energy and also how efficiently those levels are depopulated and relaxed once excitation energy is ceased.

Inherently small separations in nuclear energy states, therefore, result in weak signal-induced relaxation (depopulation of those energy levels), thus yielding low sensitivity of the MRI technique. Therefore, higher fields will yield more MR signal, and thus the signal per unit volume is larger and enables higher resolution to be achieved. However, hardware limitations and power depositions on tissue limit the field strengths and size of clinical scanners (7 or 11 Tesla), but small animal investigations can utilize even higher fields (14–17 Tesla) and improved electronics to achieve higher spatial resolution.

The natural abundance of water in microstructures in tissue helps circumvent the low MR signal sensitivity, and furthermore, alteration to the local cellular/tissue architecture is likely to reflect changes in the properties of water that can be detected by MRI. The relaxation of the excited protons is assessed by two characteristic times: spin–spin (T_2) and spin–lattice (T_1) relaxation times. Furthermore, the behavioral variations of tissue water protons in a magnetic field (e.g., diffusion of water) are also a function of molecular interactions (e.g., water and macromolecular interactions) within that environment. As the mechanisms of the T_1 and T_2 relaxation processes and other associated interactions are different, probing the desired properties during the MR acquisition time scale, whether it is by variation of timing parameters or other manipulations, enables the weighting of one or more chosen characteristic into the image.

MRI provides noninvasive insights into physiological and anatomical characteristics of a tissue. The wide array of inherent parameters and external conditions that can be varied makes

MRI a flexible modality not only to delineate anatomical details but also to probe functional behavior. The MR image, which primarily originates from tissue water, is dependent on the micro-environment of tissue, and changes in the integrity or the architecture might in turn affect the intra- and extracellular water, thereby altering qualitative or quantitative information depicted in the image.

The inherent spin–spin relaxation (T_2) is a function of the local tissue structure that could show changes once *Candida* has infiltrated the brain tissue. Among the array of timing parameters available in generating an MR image during data acquisition, parameters that affect the inherent T_2 values could be used to weigh the MR signal in the tissue to varying degrees to subsequently yield a spatial map differentiating possible damage that otherwise is hard to identify. The rate of random diffusion of water within brain tissue reflects neuronal architecture. Pathogenesis resulting from *Candida* infections can change the diffusional properties in the infected regions and is measured as diffusion coefficient. Diffusion contrast imaging can assess these changes and adds an extra dimension to understanding disease progression.

Intravascular MRI contrast agents, such as Gd-DTPA, will extravasate selectively into regions where the BBB is breached, and therefore, the measured recovery is slow in comparison to normal areas with an intact BBB. As the contrast agent affects the inherent spin–lattice (T_1) relaxation times, an appropriate T_1 weighted MRI can map the areas of damage as changes in image contrast under the influence of an appropriate imaging method. Alternatively, fast dynamic MRI scans could help map the movement of a contrast agent, which also can image changes in intensity reflecting recovery of contrast due to Gd-DTPA infusion when the BBB is breached.

The ideal evolution of the MR experiment is expected to be in an environment as homogeneous as possible. Under such condition, the loss of the MRI signal in the detecting plane is characterized by spin–spin relaxation (T_2). However, biological tissues are far from homogenous, and due the microscopic variations of magnetic fields experienced, known as magnetic susceptibility, the MRI signal detected has a different decay constant denoted as T_2^* , generally leading to image artifacts. Iron oxide (FeO) exerts paramagnetic properties in an otherwise homogeneous biological system, thus generating higher susceptibility variations. Imaging with timing parameters to enhance T_2^* effects will accentuate the susceptibility artifact that the iron oxide induces in targeted tissue. Therefore, iron oxide-based contrast agents can be employed to induce changes that affect the T_2 values. T_2^* imaging will accentuate the susceptibility artifact that the iron oxide induces in the tissue.

2 Materials

The experimental protocol, housing, and care of the mice should be in accordance with approved guidelines of the Institutional Animal care and use committee.

2.1 *Mouse Infection Model*

1. *C. albicans* wild-type (WT) strain SC5314 or any clinical strain that has shown virulence in mice can be used for mouse model studies. Genetically modified strains of *C. albicans* can be compared with WT strains that have identical auxotrophies to evaluate how potential virulence genes influence trafficking to specific target organs [9]. Alternatively, standard virulent strains of *C. albicans* can be administered to transgenic mice and WT mice to examine the role of specific host genes in pathogenesis and organ colonization.
2. For the challenge of mice, *C. albicans* cells are grown overnight in 50 mL of yeast peptone dextrose (YPD) medium at 30 °C with aeration. Higher temperatures and inclusion of media components that induce hyphal differentiation should be avoided for achieving reproducible imaging.
3. *Candida* yeast cells are harvested by centrifugation at 4200 × *g* for 10 min, washed twice with 50 mL of sterile nonpyrogenic normal saline and resuspended in 10 mL of sterile nonpyrogenic saline before quantification of the cell numbers using a counting chamber (Petroff–Hausser or hemocytometer).
4. The cell suspensions are adjusted to the final concentration for parenteral administration using nonpyrogenic sterile saline.
5. Inbred, outbred, or transgenic mouse strains can be used for these methods. Several variables must be controlled to minimize inter-animal variability in responses. Mice should be matched for age and sex, and mice from commercial vendors should be acclimated to the institutional vivarium for at least 2 weeks prior to use for imaging to minimize variation in response to *C. albicans* secondary to differences in their microbiomes.
6. An institutionally certified animal facility that can provide the required animal care and maintenance should be available.
7. Groups of five animals are placed in polycarbonate cages with stainless steel wire tops, using aspen shavings as bedding material (e.g., Harlan Teklad Laboratory Grade Sano28 Chips®, Madison, WI), and maintained on a 12-h light/dark cycle in heated, thermostatically controlled rooms for the duration of the studies.
8. The mice are fed a commercial rodent diet (e.g., 4 % Mouse/Rat Diet 7001, Harlan Teklad, Madison, WI) ad libitum. Filtered water should be provided in glass bottles fitted with stainless steel nipples mounted in rubber corks.

2.2 MRI Components

1. MRI experiments are performed on 7-T, horizontal Bruker Avance (brain) and Bruker Pharmascan (kidney) scanners (BrukerBiospin Inc., Billerica, MA, USA).
2. MagnevistW is a Food and Drug Administration-approved gadolinium diethylenetriaminepentaacetic acid (Gd-DTPA) contrast agent for MRI.
3. Macrophage and other phagocyte infiltration of the kidneys and brain are observed using ultrasmall particles of iron oxide, USPIO (Molday ION™, BIOPaL, Worcester, MA, USA).
4. The contrast agents are administered via a tail vein catheter consisting of PE10 tubing and a 30 gauge needle.
5. The anesthesia chamber consists of isoflurane (Matrx™ VIP3000 Isoflurane, Orchard Park, NY, USA) which is delivered to animals and controlled as required (*see Note 1*).
6. The in-house air mixture of medical gas (20 % O₂ and 80 % N₂) and O₂ (100 %) is delivered to the anesthesia equipment.
7. The Isoflurane/air mixture is controlled via a stop-cock assemble to first pass anesthetic to a Plexiglas setup chamber for initial knock down and subsequently to the nose cone fitted on a stereotactic cradle for MRI setup.
8. The air mixture is passed through a Capnocheck, Dual Stream EtCO₂ (BCI International, Waukesha, WI, USA), and a SAR-830 AP small animal ventilator (CWE Inc., Ardmore, PA, USA).
9. The body core temperature is maintained at 37±2 °C with a water circulating heating pad. The water heater is a Poly stat 6.5 L heated bath (Cole Palmer, IL, USA), and the rectal temperature is monitored via a Digi Sense Temp controller unit (Cole Palmer).
10. A respirator monitoring unit (Small Animal Instruments, NY, USA) consisting of a pressure transducer that lays under the abdominal cavity is used to monitor the breathing rate during Brain scans. For kidney MRI, breathing is synchronized with the MR acquisition window to minimize motion artifacts by data sampling on the ramp of each breath.
11. The radiofrequency coils used to obtain MRI images consist of two units. A larger 72 mm *i.d.* volume coil is used to induce the MR signal in the brain. The induced signal is detected with a 25 mm surface coil laid in proximity to the brain. The two coils are electronically isolated (decoupled) to avoid interactions during the role of each coil.
12. The radiofrequency coil used for kidney MRI is a 35 mm *i.d.* volume coil, which could accommodate an anesthetized mouse and plays the dual role of transmission and acquisition of the RF energy.

3 Methods

3.1 Mouse Infection with *C. albicans*

1. 8- to 12-week-old (18–20 g) mice are used for all animal experiments. Mice are randomly allocated to groups of five to six animals and housed and cared for with access to filtered water and provided standard mouse chow ad libitum. The handling and care of the animals are conducted in compliance with the guidelines established by the Animal Care and Use Committee of the Institute.
2. Each group of mice is inoculated intravenously in the lateral caudal tail vein using a 30-gauge needle with a volume of 0.1 mL containing 5×10^5 *C. albicans* cells [8]. This level of infection induces subacute candidiasis in mice with meningoencephalitis and kidney inflammation at 1, 3, and 5 days post-inoculation (dpi). Lower dose should be administered for longer term monitoring.
3. At least five mice per group at days 0, 1, 3, and 5 dpi are used to assess the level of BBB breach and inflammatory changes.
4. As the disease progresses, sick mice lose weight and show slight dehydration. Clinical signs of illness in each mouse should be evaluated three times daily, and mice that display severe signs must be euthanized immediately by CO₂ inhalation or using other euthanasia methods approved for use in the host vivarium.
5. After MRI examinations mice should be euthanized immediately by CO₂ inhalation and processed for complete necropsy and collection of tissues for histopathological examination of tissue inflammation and colonization to permit comparative studies with MRI images.

3.2 BBB Integrity Study

1. Mice are anesthetized in an induction chamber with a 30 % oxygen/70 % nitrogen (oxygen-enhanced air) gas mixture containing 5 % isoflurane. After anesthesia is induced (indicated by loss of righting reflex, decreased respiratory rate, and nonresponsiveness to toe pinch), isoflurane is reduced to 1.5–2 %, and the animals are maintained via a nose cone.
2. The catheter is introduced into the lateral tail vein, consisting of PE10 tubing and a 30 gauge needle. This facilitates administration of Gd-DTPA while in the MRI scanner.
3. Take care to allow for chest expansion to facilitate breathing. A respiratory sensor pillow is placed under the mouse or attached above to monitor the respiratory rate and pattern.
4. Mouse respiratory rate is monitored using the pressure transducer, which in turn is coupled to the acquisition software via the scanner consol. A nominal breath rate of about 60 bpm allows data acquisition with breath/data synchronization during MRI and, furthermore, seems to cause minimal stress to the animal.

5. The mouse's head needs to be centered in a 72/25-mm transmit/receive coil ensemble, and three mutually perpendicular scout images should be acquired. These pilot scans enable the positioning of the subsequent imaging slices to achieve spatial integrity.
6. T₁-weighted axial images (TR/TE=200/5.9 ms; slice thickness=1 mm; number of averages=8; matrix size=256×256; field of view (FOV)=1.92 cm) encompassing the whole brain are acquired using a gradient echo (GE) sequence, before and 5 min after the administration of a bolus of Gd-DTPA (0.2 cm³/kg body weight).
7. In order to assess the relative breaching of the BBB, analysis can be simplified by investigating selected multiple regions of interest (ROIs) in the brain placed in different regions, including the cortices of both hemispheres (Fig. 1).

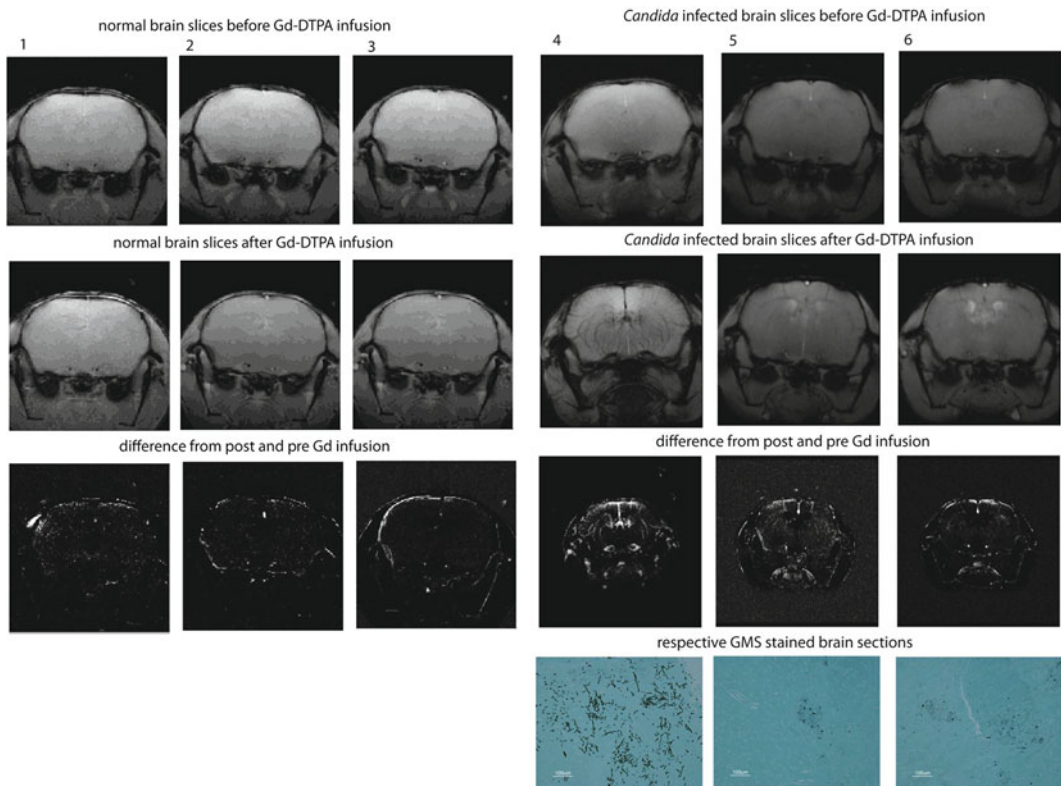


Fig. 1 MRI scans of mouse brains before (*upper panels*) and after *i.v.* administration of Gd-DTPA (*second row panels*). Gd does not penetrate the BBB in uninfected mouse brains, and thus limited changes are visible in the difference (pre-post) images (*panels 1–3, lower panels*). *C. albicans* infected mouse brains at 3 days post-inoculation show hyper-intense regions indicating BBB breaching (*panels 4–6*). GMS staining of sections obtained from the brains of the infected mice post-imaging confirms *C. albicans* colonization in the respective brains (*panels 4–6, lower panels*)

8. Further visualization of BBB integrity is achieved by dynamic contrast imaging employing an echo planar imaging (EPI) gradient echo sequence (spectral width = 350 kHz; TE = 22 ms; temporal resolution = 2 s; matrix size = 128 × 128; FOV = 1.92 cm) before, during, and after a bolus of Gd-DTPA (*see Note 2*).

3.3 Quantitative MRI

1. Average spin–spin relaxation times (T_2) and apparent diffusion coefficients (ADCs) are analyzed using a separate set of six mice per group at required intervals.
2. Nine contiguous T_2 (TE = 12 ms; 16 echoes; matrix size = 128 × 128; FOV = 1.92 cm) and diffusion (TE = 15 ms; Δ = 20 ms; b = 0,1000 mm²/s along read gradient axes; matrix size = 128 × 128; FOV = 1.92 cm) weighted axial images, originating 2 mm posterior to the olfactory bulb, should be acquired. The data are transferred offline and processed.
3. The scanned animals are then perfused under anesthesia to remove blood from the circulatory system, and the brain histology should be studied. Unless otherwise mentioned, all the MRI experimental procedures are reproduced at required intervals, utilizing at least five mice per group.

3.4 Kidney Inflammation Study Using MRI

1. Mice are anesthetized in an induction chamber with a 30 % oxygen/70 % nitrogen (oxygen-enhanced air) gas mixture containing 5 % isoflurane. After anesthesia is induced (indicated by loss of righting reflex, decreased respiratory rate, and nonresponsive to toe pinch), isoflurane is reduced to 1.5–2 %, and the animals are maintained via a nose cone.
2. For MR imaging of the region of interest, the body of the anesthetized mouse is restrained in a plastic holder with either vet wrap or tape (*see Note 3*).
3. Macrophage and other phagocyte infiltration of the kidneys and brain can be observed using USPIO (Molday IONTM, BIOPaL, Worcester, MA, USA).
4. Each mouse is given 0.015 mL of Molday ION dissolved in 0.1 mL of sterile saline, 24 h before the scan.
5. T_2^* -weighted images of the kidneys need to be acquired using a Fast Low-Angle SHot (FLASH) sequence for six mice per group at required time point and 24 h following the administration of the USPIO contrast agent, compared with control mice.
6. Thereafter, five mice representing each experimental replicate at the required time points are used for quantitative analysis at each time point to compare the progression of kidney and brain pathology.

7. After anesthesia is induced, each mouse should be positioned on a holder with its face in an anesthesia mask and its legs extended to the front and back.
8. The mice need to be centered in a 35 mm linear birdcage coil, and twelve 1 mm slices are acquired through the length of the body using a GE sequence (FOV = 5.0×3.2 cm²; TE = 10 ms; flip angle = 30; matrix size = 256×256 ; number of averages = 4).
9. In order to reduce motion artifacts, acquisition is synchronized with the breathing sensor. This yields an effective TR of approximately 1500 ms.
10. Loading with ultrasmall particles of iron oxide (USPIO) serves as a contrast agent to label phagocytes. Thus, more iron indicates more phagocytes, which in turn indicates greater inflammatory reactions in infected kidneys.

3.5 Brain Inflammation Study Using MRI

1. A separate cohort of mice is scanned on a second 7-T Bruker scanner.
2. The setup is identical to the BBB Gd study (Subheading 3.2), where the mouse's head is centered in a 72/25-mm transmit/receive coil ensemble, and three mutually perpendicular scout images are acquired.
3. T₁-weighted axial images (TR/TE = 200/5.9 ms; slice thickness = 1 mm; number of averages = 8; matrix size = 256×256 ; FOV = 1.92 cm) encompassing the whole brain were acquired using a GE sequence.

3.6 Data Analysis

1. Data from T₂, ADC, post-Gd signal variation and Dynamic contrast are analyzed using in-house software (Mathworks Inc., Natick, MA, USA).
2. T₂ and ADC contrast images are fitted to appropriate equations to evaluate respective maps, where each pixel corresponds to the local variations of the entity.
3. The blood–brain barrier breaching is computed as relative contrast ($[(\text{pre_Gd} - \text{post_Gd}) / \text{pre_Gd}] \times 100$) for a series of selected anatomical areas (ten ROIs per region in the cortex and two ROIs per region in the hippocampus, with 10 pixel areas of 5.625×10^{-4} cm²) from images obtained before and after Gd-DTPA infusion. Alternate visualization of the BBB integrity could be done by monitoring the temporal variation of the signal in dynamic contrast images. In this study two ROIs (10 pixel areas of 5.625×10^{-4} cm²) are selected in the cortex and hippocampus.

4 Notes

1. Note that isoflurane concentrations must be adjusted for some mouse strains to maintain viability and proper blood pressure.
2. Gd reduces the T1 values of mainly blood water, which yields hypo-intensities at the ROIs as the Gd flows through a given MRI slice and recovers as a sigmoid function when the BBB is intact. However, when the BBB is breached, the leaked Gd continues to yield a reduced MRI signal because the washout from those affected regions is comparatively slow.
3. Care is taken to allow for chest expansion to facilitate breathing. A respiratory sensor pillow is placed under the mouse or attached above to monitor respiratory rate and pattern. MRI may be performed for up to 3 h; however a typical anatomical scan is approximately 1 h or less.

Acknowledgements

This work was supported by the Intramural Research Program of the National Institutes of Health, National Cancer Institute, Center for Cancer Research (DDR, Z01 SC 009173), and National Institute of Neurological Disorders and Stroke (MJL).

References

1. Ashman RB (2008) Protective and pathologic immune responses against *Candida albicans* infection. *Front Biosci* 13:3334–3351
2. Navarathna DH, Nickerson KW, Duhamel GE, Jerrels TR, Petro TM (2007) Exogenous farnesol interferes with the normal progression of cytokine expression during candidiasis in a mouse model. *Infect Immun* 75:4006–4011
3. Witek-Janusek L, Shareef MJ, Mathews HL (2002) Reduced lymphocyte-mediated antifungal capacity in high-risk infants. *J Infect Dis* 186:129–133
4. Pendlebury WW, Perl DP, Munoz DG (1989) Multiple microabscesses in the central nervous system: a clinicopathologic study. *J Neuropathol Exp Neurol* 48:290–300
5. Sanchez-Portocarrero J, Perez-Cecilia E, Corral O, Romero-Vivas J, Picazo JJ (2000) The central nervous system and infection by *Candida* species. *Diagn Microbiol Infect Dis* 37:169–179
6. Hagensee ME, Bauwens JE, Kjos B, Bowden RA (1994) Brain abscess following marrow transplantation: experience at the Fred Hutchinson Cancer Research Center, 1984–1992. *Clin Infect Dis* 19:402–408
7. Borha A, Parienti JJ, Emery E, Coskun O, Khouri S, Derlon JM (2009) *Candida albicans* cerebral granuloma in an immunocompetent patient. A case report. *Neurochirurgie* 55:57–62
8. Navarathna DH, Munasinghe J, Lizak MJ, Nayak D, McGavern DB, Roberts DD (2013) MRI confirms loss of blood–brain barrier integrity in a mouse model of disseminated candidiasis. *NMR Biomed* 26:1125–1134
9. Navarathna DH, Lionakis MS, Lizak MJ, Munasinghe J, Nickerson KW, Roberts DD (2012) Urea amidolyase (DURI₂) contributes to virulence and kidney pathogenesis of *Candida albicans*. *PLoS One* 7, e48475